

Envelope excitations in electronegative plasmas with electrons featuring the Tsallis distribution

A. S. Bains* and Bo Li†

Institute of Space Sciences, Shandong University at Weihai, 264209 China

Mouloud Tribeche‡

Plasma Physics Group (PPG), Theoretical Physics Laboratory (TPL),

Faculty of Physics, University of Bab-Ezzouar,

U.S.T.H.B, B.P. 32, El Alia, Algiers 16111, Algeria.

(Dated: February 27, 2018)

Abstract

We examine the modulational instability (MI) of ion-acoustic waves (IAWs) in an electronegative plasma containing positive and negative ions as well as electrons that follow the nonextensive statistics proposed by Tsallis [J. Stat. Phys. 52, 479 (1988)]. Using the reductive perturbation method (RPM), the nonlinear Schrödinger equation (NLSE) that governs the modulational instability of the IAWs is obtained. Inspired by the experimental work of Ichiki *et al.* [Phys. Plasmas 8, 4275 (2001)], three types of electronegative plasmas are investigated. The effects of various parameters on the propagation of IAWs are discussed in detail numerically. We find that the plasma supports both bright and dark solutions. The presence of the non-extensively distributed electrons is found to play a crucial role in the formation of envelope excitations. The region in the parameter space where the MI exists depends sensitively on the positive to negative ion mass ratio (M) and negative to positive ion density ratio (ν). An extensive range of the nonextensive q -parameters ($-1 < q < 3$) is considered and in each case the MI sets in under different conditions. The finding of this investigation is useful for understanding stable wave propagation of envelope ion-acoustic solitary waves in space and laboratory plasmas comprising ions with both positive and negative charges as well as non-Maxwellian electrons.

*Electronic address: bainsphysics@yahoo.co.in.

†Electronic address: bbl@sdu.edu.cn

‡Electronic address: mtribeche@usthb.dz

I. INTRODUCTION

Electronegative plasmas, namely, plasmas comprising an appreciable amount of negative ions, have been found in a wide variety of astrophysical environments. These include the Earth's ionosphere [1] and mesosphere [2], cometary comae [3], and the Titan's ionosphere [4], to name but a few. Equally important is that electronegative plasmas exhibit many technological applications such as neutral beam sources [5], plasma processing reactors [6], synthesis of nanomaterials [7], and semiconductor materials processing [8]. Due to its wide application in laboratory and space plasmas, many authors studied wave propagation phenomena in such plasma systems [9–14].

There are many circumstances in which the well-known Maxwellian distribution proves not to be a proper description of the plasma species [15–17]. Rather, the so-called superthermal or Tsallis distribution, seems common to the species in general [18–21], and the electrons in particular [22–25]. As is well-known, the Maxwellian distribution in the Boltzmann-Gibbs statistics is believed to be universally valid for macroscopic ergodic equilibrium systems. However, for such systems as plasmas and gravitational systems where long-range interactions are present and where non-equilibrium stationary states exist, the Maxwellian distribution may be inadequate. For this reason, a large number of theoretical investigations have been made into the nonextensive statistic mechanics based on the deviations from the Boltzmann-Gibbs-Shannon (B-G-S) entropic measure. A suitable nonextensive generalization of the B-G-S entropy for statistical equilibrium was first recognized by Renyi [26] and subsequently proposed by Tsallis [27], suitably extending the standard additivity of entropy to the nonlinear, nonextensive case where one particular parameter, the entropic index q , characterizes the degree of nonextensivity of the considered system. When $q = 1$, one recovers the standard, extensive, B-G-S statistics. This non-additive entropy of Tsallis and the ensuing generalized statistics have been employed with success in a wide range of phenomena characterized by nonextensivity [28–42, 46]. Specifically, a growing body of observational evidence in astrophysical environments suggests that the q -entropy provides a convenient framework for the analysis of stellar polytropes [43], the solar neutrino problem [44], and peculiar velocity distribution of galaxy clusters [45]. Likewise, there are experimental results for electrostatic plane-wave propagation in a collisionless thermal plasma that point to a class of Tsallis's velocity distribution described by a nonextensive

q -parameter smaller than unity[46].

The deviation of the velocity distribution functions (VDFs) of plasma species from a Maxwellian has proven to have a profound effect on the nonlinear collective phenomena in many environments[47]. It is then no surprise that the q -nonextensive description is becoming increasingly popular as far as the studies of solitary waves in plasmas where the electron VDF is not a Maxwellian are concerned[48–50]. For instance, Saini *et al.*[51] studied Ion-Acoustic Waves (IAWs) with arbitrary amplitudes in the presence of superthermal electrons and obtained existence conditions for and some characteristics of IAWs in a plasma composed of cold ions and kappa-distributed electrons. Likewise, Boubakour *et al.*[52] examined such IAWs in a plasma comprising inertial ions, Maxwellian positrons and superthermal electrons, and showed that the superthermality of the electrons influences substantially the profile of the solitons. Recently, Tribeche *et al.* [48] studied the characteristics of ion-acoustic solitary waves in a two-component plasma with a q -nonextensive electron velocity distribution. Also, modulational instability of different modes in several plasma environments has been studied [53–57].

Surprisingly, most of the above-mentioned papers are restricted to two species plasmas, and only a few investigations are concerned with electronegative plasmas. Among them, Elwaskil *et al.*[10] studied the envelope excitations of solitary waves in a system with the combination of (H^+, O_2^-) or (H^+, H^-) together with nonthermal electrons whose distribution is described by the Cairns scheme [58]. The model supported both bright-(pulses) and dark-(holes, voids) solitons. Very recently, Taibany and Tribeche [59] studied weak solitary structures in electronegative plasma with nonextensive velocity distribution. They derived the Korteweg-de Vries (KdV) equation which describes the evolution of an unmodulated wave, a bare pulse containing no high frequency oscillation inside the wave packet. It was observed that the nonextensivity of electrons and the positive to negative ion mass ratio significantly change the velocity, amplitude and width of the solitary waves.

The aim of the present study is to extend the work of Taibany and Tribeche [59], and examine the combined effect of nonextensively distributed electrons and negative ions on the modulational instability (MI) of ion-acoustic waves. For this we derive the nonlinear Schrodinger equation (NLSE) that describes the evolution of the modulated wave packet. In the NLSE, the nonlinearity is in balance with the group velocity dispersion and the resulting stationary solutions have envelope structures. The organization of this paper is as follows.

In section II, we present the basic equations for an electronegative plasma and carry out a reductive perturbation to derive the appropriate nonlinear Schrödinger equation (NLSE). The modulational instability is discussed in Sec.III. and our findings are summarized in Sec.IV.

II. BASIC EQUATIONS

We consider a plasma model whose constituents are singly charged fluid cold positive ions (subscript p), singly charged fluid cold negative ions (subscript n), and nonextensive electrons (subscript e). The nonlinear dynamics of ion-acoustic oscillations is governed by the following normalized equations [59]:

-for positive ions

$$\frac{\partial n_p}{\partial t} + \frac{\partial n_p v_p}{\partial x} = 0, \quad (1)$$

$$\frac{\partial u_p}{\partial t} + v_p \frac{\partial v_p}{\partial x} + \frac{\partial \phi}{\partial x} = 0, \quad (2)$$

-for negative ions

$$\frac{\partial n_n}{\partial t} + \frac{\partial n_n v_n}{\partial x} = 0, \quad (3)$$

$$\frac{\partial u_n}{\partial t} + v_n \frac{\partial v_n}{\partial x} - M \frac{\partial \phi}{\partial x} = 0, \quad (4)$$

-Poisson equation

$$\frac{\partial^2 \phi}{\partial x^2} = n_n - n_p + n_e \quad (5)$$

where the expression for the nonextensive electron density is given by [49, 55]

$$n_e = \mu [1 + (q - 1)\phi]^{(q+1)/2(q-1)} \quad (6)$$

In Eqs. (1) - (6), $n_{p,n}$ is the ion number density normalized by the unperturbed positive ion density n_{p0} , $u_{p,n}$ is the ion fluid velocity normalized by the ion sound speed $C_s = (k_B T_e / m_p)^{1/2}$, and ϕ is the electrostatic wave potential normalized by $k_B T_e / e$. The time t is normalized by the ion plasma period $\omega_{pi}^{-1} = (4\pi e^2 n_{p0} / m_i)^{-1/2}$, and the space variable x is in unit of the ion Debye length $\lambda_{Di} = (k_B T_e / 4\pi e^2 n_{p0})^{1/2}$. Here k_B is the Boltzmann constant, T_e is the electron temperature, and e is the electron charge. We define the mass ratio M as m_p / m_n where m_p (m_n) is the positive (negative) ion mass. The

neutrality condition implies $\nu + \mu = 1$, where $\nu = n_{n0}/n_{p0}$ and $\mu = n_{e0}/n_{p0}$. Moreover, the parameter q stands for the strength of the electron nonextensivity. For $q < -1$, the nonextensive electron distribution is unnormalizable. In the extensive limiting case $q \rightarrow 1$, the electron density, Eq. (6), reduces to its well-known Maxwell-Boltzmann counterpart.

To investigate the modulation of the IAWs, we employ the standard reductive perturbation technique (RPT) to derive the appropriate nonlinear Schrödinger equation (NLSE). The independent variables are stretched as $\xi = \epsilon(x - v_g t)$ and $\tau = \epsilon^2 t$, where ϵ is a small parameter and v_g the group velocity of the wave. The dependent variables are then expanded as

$$\begin{aligned}
n_p &= 1 + \sum_{m=1}^{\infty} \epsilon^m \sum_{l=-\infty}^{+\infty} n_{pl}^m(\xi, \tau) e^{i l(kx - \omega t)}, \\
n_n &= \nu + \sum_{m=1}^{\infty} \epsilon^m \sum_{l=-\infty}^{+\infty} n_{nl}^m(\xi, \tau) e^{i l(kx - \omega t)}, \\
u_{p,n} &= \sum_{m=1}^{\infty} \epsilon^m \sum_{l=-\infty}^{+\infty} u_{p,nl}^m(\xi, \tau) e^{i l(kx - \omega t)}, \\
\phi &= \sum_{m=1}^{\infty} \epsilon^m \sum_{l=-\infty}^{+\infty} \phi_l^m(\xi, \tau) e^{i l(kx - \omega t)}. \tag{7}
\end{aligned}$$

For $n_{p,n}$, $u_{p,n}$ and ϕ to be real, one requires that $A_{-l}^m = (A_l^m)^*$ where the asterisk denotes complex conjugate. Substituting these expressions along with the stretching coordinates into Eqs. (1)-(5) and collecting the terms in the different powers of ϵ , we can obtain the m -th order reduced equations. At the first order ($m = 1$), we can obtain for $l = 1$ the first-order quantities in terms of $\phi_1^{(1)}$ as

$$\begin{aligned}
-i\omega n_{p1}^{(1)} + ik u_{p1}^{(1)} &= 0, & -i\omega u_{p1}^{(1)} + ik \phi_1^{(1)} &= 0, \\
-i\omega n_{n1}^{(1)} + i\nu k u_{p1}^{(1)} &= 0, & -i\omega u_{n1}^{(1)} - ik M \phi_1^{(1)} &= 0, \\
n_{p1}^{(1)} - n_{n1}^{(1)} - (k^2 + c_1) \phi_1^{(1)} &= 0, \tag{8}
\end{aligned}$$

where $c_1 = \mu(q + 1)/2$.

The solution for the first harmonics is

$$n_{p1}^{(1)} = \frac{k^2}{\omega^2} \phi_1^{(1)}, \quad u_{p1}^{(1)} = \frac{k}{\omega} \phi_1^{(1)}, \quad n_{n1}^{(1)} = -\nu M \frac{k^2}{\omega^2} \phi_1^{(1)}, \quad u_{n1}^{(1)} = -M \frac{k}{\omega} \phi_1^{(1)} \tag{9}$$

Thus, we obtain the following dispersion relation for IAWs

$$\frac{\omega^2}{k^2} = \frac{1 + \nu M}{(k^2 + c_1)}. \quad (10)$$

Figure 1 presents the solution to the dispersion relation in the form of ω as a function of k at different values of the positive to negative mass ratio M . It is observed that ω increases with increasing k . Furthermore, ω decreases with increasing M . This means that increasing M decreases the energy as well as the oscillations of the wave.

At the second order ($m = 2$) and for $l = 1$, the following equations are obtained

$$-\iota\omega n_{p1}^{(2)} + \iota k u_{p1}^{(2)} = v_g \frac{\partial n_{p1}^{(1)}}{\partial \xi} - \frac{\partial u_{p1}^{(1)}}{\partial \xi}, \quad (11)$$

$$-\iota\omega u_{p1}^{(2)} + \iota k \phi_1^{(2)} = v_g \frac{\partial u_{p1}^{(1)}}{\partial \xi} - \frac{\partial \phi_1^{(1)}}{\partial \xi}, \quad (12)$$

$$-\iota\omega n_{n1}^{(2)} + \iota k \nu u_{n1}^{(2)} = v_g \frac{\partial n_{n1}^{(1)}}{\partial \xi} - \nu \frac{\partial u_{n1}^{(1)}}{\partial \xi}, \quad (13)$$

$$-\iota\omega u_{n1}^{(2)} - \iota k M \phi_1^{(2)} = v_g \frac{\partial u_{n1}^{(1)}}{\partial \xi} + M \frac{\partial \phi_1^{(1)}}{\partial \xi}, \quad (14)$$

$$(k^2 + c_1)\phi_1^{(2)} + n_{n1}^{(2)} - n_{p1}^{(2)} = 2\iota k \frac{\partial \phi_1^{(1)}}{\partial \xi}, \quad (15)$$

along with the compatibility condition

$$v_g = \frac{c_1}{(1 + \nu M)} \frac{\omega^3}{k^3}. \quad (16)$$

If we proceed further in the same way as in Ref. [60], and substitute the derived expressions for $m = 2$, $l = 0$ and $m = 2$, $l = 2$ into the components for $m = 3$, $l = 1$ of the reduced equations, we can obtain the following nonlinear Schrodinger equation

$$\iota \frac{\partial \phi_1^{(1)}}{\partial \tau} + P \frac{\partial^2 \phi_1^{(1)}}{\partial \xi^2} + Q |\phi_1^{(1)}|^2 \phi_1^{(1)} = 0 \quad (17)$$

where

$$P = \frac{1}{2} \frac{d^2 \omega}{dk^2} = -\frac{3}{2} \frac{c_1}{(1 + \nu M)^2} \frac{\omega^5}{k^4} \quad (18)$$

and

$$Q = \frac{\omega^3}{2k^2} \left[3c_3 - 2c_2(A_\phi + B_\phi) - 2\frac{k^3}{\omega^3}(A_{up} + B_{up}) - \frac{k^2}{\omega^2}(A_{np} + B_{np}) - 2\nu M \frac{k^3}{\omega^3}(A_{un} + B_{un}) - M \frac{k^2}{\omega^2}(A_{nn} + B_{nn}) \right] \quad (19)$$

where

$$\begin{aligned} A_\phi &= \frac{(1 - \nu M^2) \frac{3k^4}{2\omega^4} + c_2}{(c_1 + 4k^2) - (1 - \nu M) \frac{k^2}{\omega^2}}, \\ B_\phi &= \frac{v_g^2 \left(2c_2 + (1/v_g + 2k/\omega) \frac{(1 - \nu M^2)k^2}{v_g \omega^2} \right)}{v_g^2 c_1 - (1 + \nu M)}, \\ A_{up} &= A_\phi \frac{k}{\omega} + \frac{k^3}{2\omega^3}, \quad A_{np} = A_{up} \frac{k}{\omega} + \frac{k^4}{\omega^4}, \\ A_{un} &= -M A_\phi \frac{k}{\omega} + \frac{M^2 k^3}{2\omega^3}, \quad A_{nn} = A_{un} \frac{\nu k}{\omega} + \frac{\nu M^2 k^4}{\omega^4}, \\ B_{up} &= \frac{B_\phi}{v_g} + \frac{k^2}{v_g \omega^2}, \quad B_{np} = \frac{B_{up}}{v_g} + \frac{2k^3}{v_g \omega^3}, \\ B_{un} &= -B_\phi \frac{M}{v_g} + \frac{M^2 k^2}{v_g \omega^2}, \quad B_{nn} = B_{un} \frac{\nu}{v_g} + \frac{2\nu M^2 k^3}{v_g \omega^3} \\ c_2 &= \frac{(q+1)(q-3)}{8}, \quad c_3 = \frac{(q+1)(q-3)(3q-5)}{48} \end{aligned} \quad (20)$$

III. NUMERICAL ANALYSIS

Let us now investigate the stability/instability of the modulated wave packets in an electronegative plasma with nonextensive electrons on the basis of the NLSE (17) that governs the MI of the IAWs. Based on the linear stability analysis [61], it is observed that the wave is modulationally unstable when $PQ > 0$ in the modulation wave number region $k^2 < \frac{2Q}{P} |\phi_0|^2$, where ϕ_0 is the amplitude of the carrier waves. Furthermore, the maximum growth rate is given by $Q |\phi_0|^2$ and is attained at $k = \sqrt{\frac{Q}{P}} |\phi_0|$. Two types of stationary solutions are possible: (i) bright envelope soliton when $PQ > 0$ and (ii) dark envelope soliton when $PQ < 0$. For unstable wave packets ($PQ > 0$), we have envelope solitons given by

$$\phi = \sqrt{\left| \frac{2\gamma}{Q} \right|} \operatorname{sech} \left(\left| \frac{\gamma}{P} \right| \zeta \right) e^{i\gamma\tau}, \quad (21)$$

where γ is a real constant. For stable wave packet ($PQ < 0$), we obtain a modulationally stable ion-acoustic mode with special solution known as envelope dark soliton given by

$$\phi = \sqrt{\left|\frac{\gamma}{Q}\right|} \tanh\left(\left|\frac{\gamma}{2P}\right|\zeta\right) e^{\nu\gamma\tau}. \quad (22)$$

It is obvious from Eqs.(21) and (22) that the width and the amplitude of the solitary wave vary with P and Q . The soliton width is proportional to $|P|$ and the soliton amplitude is inversely proportional to $|Q|$. These coefficients in turn depend upon a number of parameters such as positive to negative ion mass ratio M , negative to positive ion density ratio ν and the electron nonextensive parameter q . Consequently, one expects that these parameters would affect the stability criteria over a wide range in the parameters space.

To proceed further, some specific applications are necessary for a quantitative analysis to be made. To this end, we focus on the following four types of plasmas [62]: ($\text{Xe}^+\text{-F}^-$) with $M = 131/19 \simeq 6.89$, ($\text{Ar}^+\text{-F}^-$) with $M = 40/19 \simeq 2.10$, ($\text{Xe}^+\text{-SF}_6^-$) with $M = 131/146 \simeq 0.89$ and ($\text{Ar}^+\text{-SF}_6^-$) with $M = 40/146 \simeq 0.27$. Evaluating the dispersive coefficient P , we find that for all sets of parameters, P is always negative. Hence, the conditions for instability is determined by the sign of the nonlinear coefficient Q .

Figure 2 displays the variation of the nonlinear coefficient Q for different types of plasmas. It is clear from this plot that Q has different trends for the different types of plasmas. For higher values of positive to negative ion mass ratio M , the nonlinear coefficient is negative for small k and becomes positive for larger values of k . As M decreases, Q starts to change its sign towards positive values for small wave numbers. The behavior is totally different when $M < 1$, for the $\text{Xe}^+\text{-SF}_6^-$ and $\text{Ar}^+\text{-SF}_6^-$ plasmas. In this case the nonlinear coefficient Q is positive for small values of k , but turns negative beyond a certain k .

Given that P is negative definite for all the parameters considered, the product PQ has different trends for different types of plasmas as well. It follows that the stability profile may be readily obtained by examining the ratio P/Q against k . The wavenumber k corresponding to $Q = 0$ is of particular relevance since it is the critical or threshold wavenumber for the onset of the MI. For the ease of description, it will be termed k_c .

For the $\text{Xe}^+\text{-F}^-$ plasma, the variation of P/Q as a function of k for different values of the nonextensive parameter q is shown in Fig.3. One notices that both unstable and stable regions are obtained. The amplitude remains unstable when $k < k_c$ and becomes stable when the opposite is true. Bright solitons occur in the former case and therefore correspond

to large wavelengths, whereas dark envelope solitons occur in the latter region. Besides, it can be seen that the critical value k_c , where the instability sets in, increases when q increases, meaning that for vanishingly small $q \rightarrow 1$, the MI occurs at small wavelengths.

The combined effect of negative to positive ion ratio (ν) and the electron nonextensivity for $M = 6.89$ is depicted in Fig.4. It is clear that the critical wavenumber k_c decreases with increasing μ , namely, with the decrease in the negative to positive ion density ratio. In other words, the more negative ions that are introduced into the plasma, the smaller the wavelength beyond which the instability sets in will be. For a fixed value of μ , the critical wavenumber k_c increases sharply in the region $-0.9 < q < 0$. As $q \rightarrow 1$, i.e., as the distribution approaches a Maxwellian, k_c acquires an almost saturated value.

With μ fixed, the variation of P/Q as a function of k for an $\text{Ar}^+\text{-F}^-$ plasma ($M = \frac{40}{19} \simeq 2.10$) is shown in Fig.5. Qualitatively similar behaviors are obtained as earlier, and both unstable and stable regions are obtained. The amplitude is unstable at large wavelengths and becomes stable as the wavelength drops below a certain value. The electron nonextensivity has an interesting effect on the instability profile now. The critical wavenumber k_c increases for negative values of q . However, a further increase in the q -parameter decreases k_c . As the distribution approaches a Maxwellian the stability/instability occurs at small k .

This picture is clearer in Fig.6, where the critical wavenumber k_c is plotted as a function of q for different values of μ . At any given value of q , it is seen that with an increase in μ , the critical value decreases, just like in the previous case. The amplitude is unstable at small k , and the critical wavenumber at which the transition occurs increases in the region $-0.9 < q < -0.5$. After that, the critical number continuously decreases with increasing q .

In the two plasmas we have discussed so far, the amplitude is unstable at small k (large wavelength) and becomes stable at large k . The results are very different from earlier investigations, due to large values of M . The available studies have not examined the case where $M > 1$. The maximum value of $M = 1$ is taken by Elwaskil *et al.* [10] for a $\text{H}^+\text{-H}^-$ plasma. So it is worth mentioning here that M has significant effect on the formation of envelope solitons, *i.e.*, if we take $M > 1$ the results are opposite to the case for $M < 1$.

Now we proceed to the $\text{Xe}^+\text{-SF}_6^-$ and $\text{Ar}^+\text{-SF}_6^-$ plasmas, where $M < 1$. It turns out that the results are in many ways distinct from what we found. The effect of the electron nonextensivity on the modulational instability in the case of the $\text{Xe}^+\text{-SF}_6^-$ plasma is studied in detail in Figs.7 and 8. The former, which depicts the ratio P/Q as a function of k for

different values of q , at a given value of μ displays such an influence. Although both dark and bright excitations are possible, as in the previous cases, what is distinct now is that the wave is stable for small k , but modulationally unstable at large k . The critical wavenumber k_c at which the instability sets in first increases and then decreases for different ranges of q . The electron nonextensivity plays therefore a crucial role in the characterization of localized envelope excitations in different plasma environments. This point is better illustrated in Fig.8, in which a wide range of q together with a number of μ are explored. Note that the critical wavenumber k_c behaves in different manners in different ranges of the nonextensive parameter q . For $q < -0.5$, the critical wavenumber increases with increasing μ . However, as $q \rightarrow 1$, the critical value decreases with increasing μ . This means that adding more negative ions into the system leads to instability at larger k . Similar results (not shown) are obtained in the case of the $\text{Ar}^+\text{-SF}_6^-$ plasma for which $M = 0.27$. The amplitude is stable for small wavenumbers and becomes unstable at large k . The critical wavenumber for instability first increases and then decreases with an increase in the q parameter.

IV. CONCLUSION

To conclude, we have investigated the modulational instability (MI) of ion-acoustic waves (IAWs) in an electronegative plasma where both positively and negatively charged ions are present, and where the electrons are described within the theoretical framework of the nonextensive statistics proposed by Tsallis [27]. Using the reductive perturbation method (RPM), the nonlinear Schrödinger equation (NLSE) that governs the modulational instability of the IAWs is obtained. Inspired by the experimental work of Ichiki *et al.* [62], four types of electronegative plasmas are examined, which differ mainly in the positive to negative ion mass ratio. The effects of various parameters on the propagation of the IAWs are discussed in detail numerically. It is found that the plasma supports both bright as well as dark solitons. We find that the presence of the nonextensive electrons plays a crucial role in the formation of the envelope excitations. The region of modulational instability is significantly affected by the positive to negative ion mass ratio (M), and the negative to positive ion density ratio (ν). An extensive range of the nonextensive q -parameter is considered and in each case the MI sets in under different conditions. The findings of this investigation are useful in understanding stable wave propagation of envelope ion-acoustic solitary waves in space and

laboratory plasmas where two type of ions and non-Maxwellian electrons are present.

Acknowledgments

This research is supported by the National Natural Science Foundation of China (40904047, 41174154, and 41274176), the Ministry of Education of China (20110131110058 and NCET-11-0305), and by the Provincial Natural Science Foundation of Shandong via Grant JQ201212.

-
- [1] H. Massey, *Negative Ions*, 3rd ed. (Cambridge University Press, Cambridge, 1976), p. 663.
 - [2] C. F. del Pozo, E. Turunen, and T. Ulich, *Ann. Geophys.*, **17**, 782-793, (1999)
 - [3] P. H. Chaizy, H. Re'me, J. A. Sauvaud, C. D'uston, R. P. Lin, D. E. Larson, D. L. Mitchell, K. A. Anderson, C. W. Carlson, A. Korth, and D. A. Mendis, *Nature (London)* **349**, 393 (1991).
 - [4] A. J. Coates, F. J. Crary, G. R. Lewis, D. T. Young, J. H. Waite, Jr., and E. C. Sittler Jr., *Geophys. Res. Lett.* **34**, L22103, (2007).
 - [5] M. Bascal and G. W. Hamilton, *Phys. Rev. Lett.* **42**, 1538 (1979).
 - [6] R. A. Gottscho and C. E. Gaebe, *IEEE Trans. Plasma Sci.* **14**, 92 (1986).
 - [7] H. Kokura, S. Yoneda, K. Nakamura, N. Mitsuhiro, M. Nakamura, and
 - [8] H. Sugai, *Jpn. J. Appl. Phys.* **38**(Part 1), 5256 (1999).
 - [9] T. S. Gill, H. Kaur and N. S. Saini, *Phys. Plasmas*, **10**, 3927 (2003).
 - [10] S. A. Elwaskil, E. K. El-Shewy and H. G. Abdelwahed, *Phys. Plasmas* **17**, 052301 (2010).
 - [11] S. Ghosh, S. Sarkar, M. Khan and M. R. Gupta. *Phys. Rev E*, **84**, 066401 (2011).
 - [12] T. Akhter, M.M. Hossain and A.A. Mamun, *Astrophys. Space Sci.* **345**, 283 (2013).
 - [13] W. F. El-Taibany, N. A. El-Bedwehy, and E. F. El-Shamy, *Phys. Plasmas* **18**, 033703 (2011).
 - [14] S. K. El-Labany, W. M. Moslem, Kh. A. Shnishin, S. A. El-Tantawy, and P. K. Shukla, *Phys. Plasmas* **18**, 042306 (2011).
 - [15] S. P. Christon, D. G. Mitchell, D. J. Williams, L. A. Frank, C. Y. Huang, and T. E. Eastman, *J. Geophys. Res.* **93**, 2562, (1988).
 - [16] M. Maksimovic, V. Pierrard, and P. Riley, *Geophys. Res. Lett.* **24**, 1511, (1997).
 - [17] M. P. Leubner, *Phys. Plasmas* **11**, 1308 (2004).

- [18] N. S. Saini and I.Kourakis, Phys. Plasmas, 15, 123701 (2008).
- [19] P. Eslami, M. Mottaghizadeh, H. R. Pakzad, Phys. Plasmas 18, 102303 (2011).
- [20] S. A. El-Tantawy, N. A. El-Bedwehy and W. M. Moslem, Phys. Plasmas, 18 052113 (2011).
- [21] J. Borhanian and M. Shahmansouri, Phys. Plasmas 20 013707 (2013)
- [22] H. R. Pakzad, Phys. Plasmas. 18, 082105 (2011).
- [23] P. Eslami, M. Mottaghizadeh, H. R. Pakzad, Phys. Plasmas 18, 102313 (2011).
- [24] S. A. Shan and A. Mushtaq, Phy. Scr. 86, 035503 (2012).
- [25] D. K. Ghosh, P. Chatterjee and U. G. Narayan, Phys. Plasmas, 19, 033703 (2012).
- [26] A. Renyi, Acta Math. Hungaria **6**, 285 (1955).
- [27] C. Tsallis, J. Stat. Phys. **52**, 479 (1988).
- [28] R. Rossignoli and N. Canosa, Phys. Lett. A **264**,148 (1999).
- [29] A. R. Lima, J. S. Sá Martins, and T. J. P. Penna, Physica A **268**, 553 (1999).
- [30] A. V. Milovanov and L. M. Zelenyi, Nonlin. Processes Geophys. **7**, 211 (2000).
- [31] S. Abe, S. Martinez, F. Pennini, and A. Plastino, Phys. Lett. A **281**, 126 (2001).
- [32] G. Kaniadakis, Phys. Lett. A **288**, 283 (2001).
- [33] A. Lavagno, Phys. Lett. A **301**, 13 (2002).
- [34] T. Wada, Phys. Lett. A **297**, 334 (2002).
- [35] A. M. Reynolds and M. Veneziani, Phys. Lett. A **327**, 9 (2004).
- [36] J. Du, Phys. Lett. A **320**, 347 (2004).
- [37] F. Sattin, Phys. Scr. **71**, 443 (2005).
- [38] V. Muñoz, Nonlin. Processes Geophys. **13**, 237 (2006).
- [39] J. Wu and H. Chen, Phys. Scr. **75**, 722 (2007).
- [40] M. P. Leubner, Nonlin. Processes Geophys. **15**, 531 (2008).
- [41] R. Hanel and S. Thurner, Phys. Lett. A **373**, 1415 (2009).
- [42] R. Amour and M. Tribeche, Phys. Plasmas **17**, 063702 (2010).
- [43] A. R. Plastino and A. Plastino, Phys. Lett. A **174**, 384 (1993).
- [44] G. Kaniadakis, A. Lavagno, and P. Quarati, Phys. Lett. B **369**, 308 (1996).
- [45] A. Lavagno, G. Kaniadakis, M. Rego-Monteiro, P. Quarati, and C. Tsallis, Astrophys. Lett. Commun. **35**, 449 (1998).
- [46] J. A. S. Lima, R. Silva, Jr., and J. Santos, Phys. Rev. E **61**, 3260 (2000).
- [47] D. Summers and R. M. Thorne, Phys. Fluids B **3**, 1835 (1991).

- [48] M. Tribeche, L. Djebarni, R. Amour, Phys. Plasmas **17** 042114 (2010).
- [49] M. Tribeche and L. Djebarni, Phys. Plasmas **17**, 124502 (2010).
- [50] S. Ali Shan and N. Akhtar, Astrophys. Space Sci. **346**, 367 (2013).
- [51] N. S. Saini, I. Kourakis and M. A. Hellberg, Phys. Plasmas. **16**, 062903 (2009).
- [52] N. Boubakour, M. Tribeche and K. Aoutou, Phys. Scr. **79** 065503 (2009).
- [53] T. S. Gill, A. S. Bains and C. Bedi, Phys. Plasmas **17**, 013701 (2010).
- [54] T. S. Gill, C. Bedi and A. S. Bains, Phys. Scr. **81** 055503 (2010).
- [55] A. S. Bains, M. Tribeche and T. S. Gill, Phys. Plasmas, **18**, 022108 (2011).
- [56] A. S. Bains, M. Tribeche and T. S. Gill, Phys. Letters A, **375**, 2059 (2011).
- [57] A. S. Bains, M. Tribeche and C. S. Ng, Astro. Space Sci. **343**, 621 (2013).
- [58] R.A. Cairns, A.A. Mamun, R. Bingham, R. Boström, R.O. Dendy, C.M.C. Nairn, P.K. Shukla, Geophys. Res. Lett. **22**, 2709 (1995).
- [59] W. F. El Taibany and Tribeche Phys. Plasmas **19**, 024507 (2012).
- [60] I. Kourakis and P. K. Shukla, Nonlinear Process. Geophys. **12**, 407 (2005).
- [61] M. R. Amin, G. E. Morfill, P. K. Shukla: Phys. Rev. E, **58**, 6517 (1998).
- [62] R. Ichiki, M. Shindo, S. Yoshimura, T. Watanabe, and Y. Kawai, Phys. Plasmas **8**, 4275 (2001).

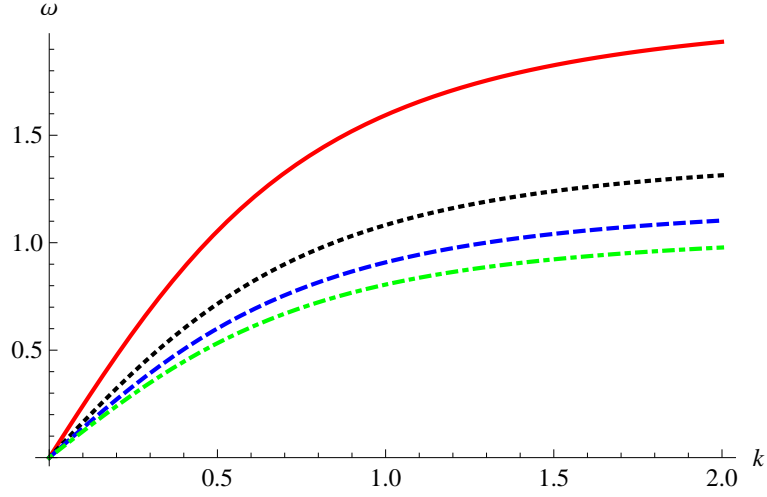


FIG. 1: (Color online) Variation of the carrier frequency ω with the wave number k for different types of plasmas with $\mu = 0.5$ and $q = 0.5$. Solid curve corresponds to $Xe^+ - F^-$ plasma ($M = \frac{131}{19} \simeq 6.89$); dotted curve to $Ar^+ - F^-$ plasma ($M = \frac{40}{19} \simeq 2.10$), dashed curve to $Xe^+ - SF_6^-$ plasma ($M = \frac{131}{146} \simeq 0.89$) and dotted dashed curve to $Ar^+ - SF_6^-$ plasma ($M = \frac{40}{146} \simeq 0.27$).

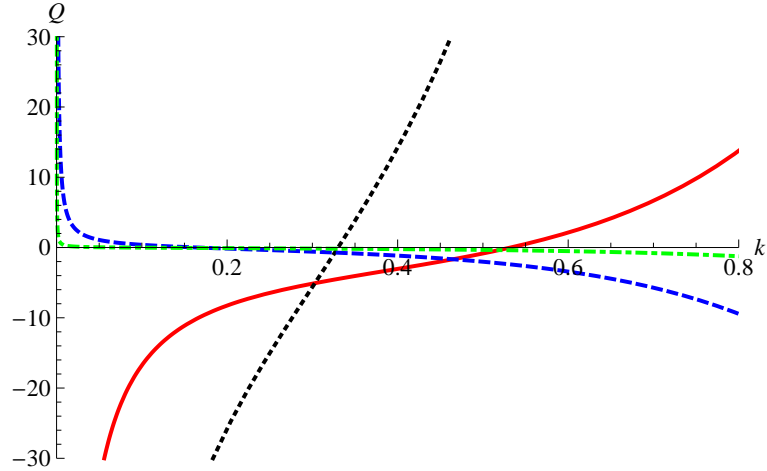


FIG. 2: (Color online) Variation of the NLSE coefficient Q with the carrier wave number k for different types of plasmas with $\mu = 0.5$ and $q = 0.5$. Solid curve corresponds to $Xe^+ - F^-$ plasma ($M = \frac{131}{19} \simeq 6.89$); dotted curve to $Ar^+ - F^-$ plasma ($M = \frac{40}{19} \simeq 2.10$), dashed curve to $Xe^+ - SF_6^-$ plasma ($M = \frac{131}{146} \simeq 0.89$) and dotted dashed curve to $Ar^+ - SF_6^-$ plasma ($M = \frac{40}{146} \simeq 0.27$).

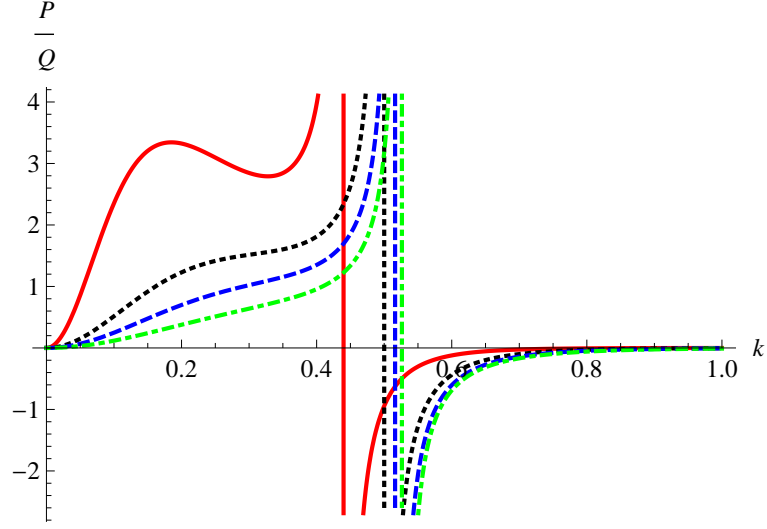


FIG. 3: (Color online) Variation of the ratio P/Q with the carrier wave number k for different values of the q -nonextensive parameter with $\mu = 0.5$ for $Xe^+ - F^-$ plasma ($M = \frac{131}{19} \simeq 6.89$). Solid curve corresponds to $q = -0.7$; dotted curve to $q = -0.3$; dashed curve to $q = 0$ and dotted-dashed curve to $q = 0.4$.

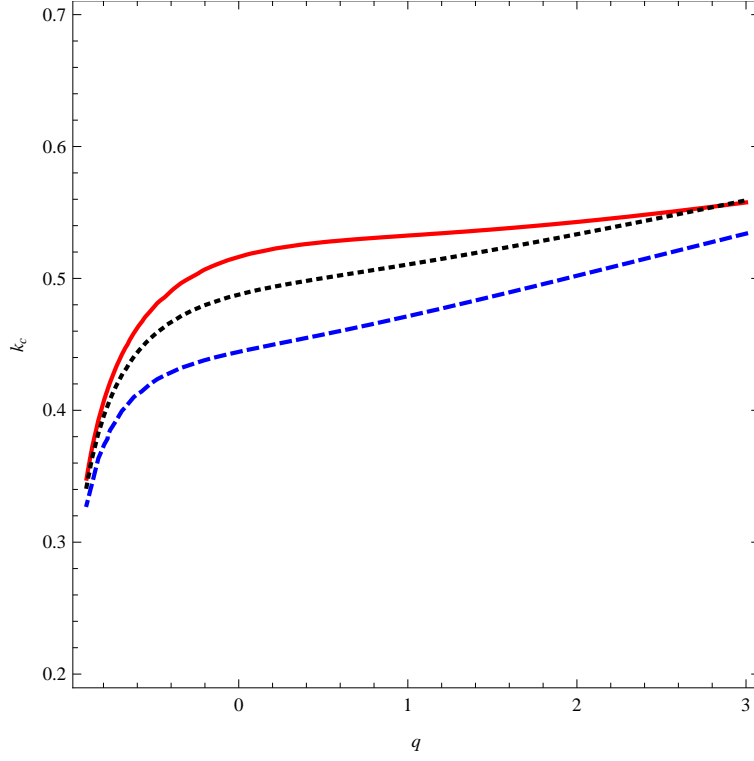


FIG. 4: (Color online) Variation of the critical wave number k_c with the q -nonextensive parameter for different values of μ with $M = 6.89$. Solid curve corresponds to $\mu = 0.5$; dotted curve to $\mu = 0.6$ and dashed curve to $\mu = 0.7$.

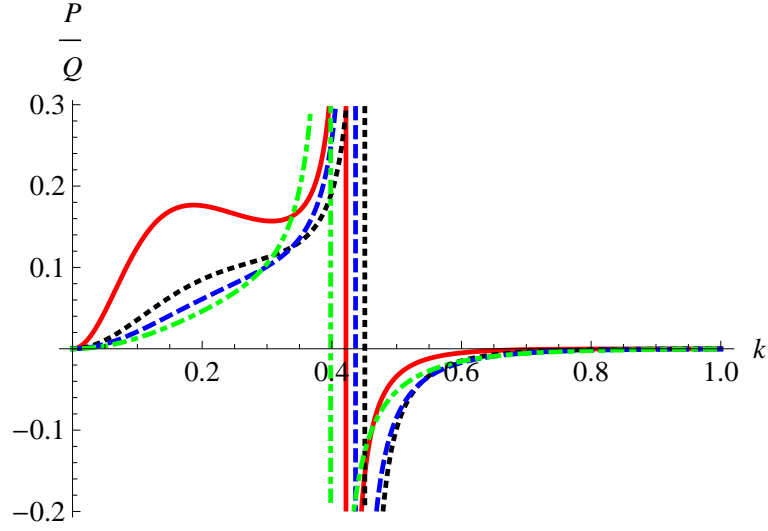


FIG. 5: (Color online) Variation of the ratio P/Q with the carrier wave number k for different values of the q -nonextensive parameter with $\mu = 0.5$ for the $Ar^+ - F^-$ plasma ($M = \frac{40}{19} \simeq 2.10$). Solid curve corresponds to $q = -0.7$; dotted curve to $q = -0.3$; dashed curve to $q = 0$ and dotted-dashed curve to $q = 0.4$.

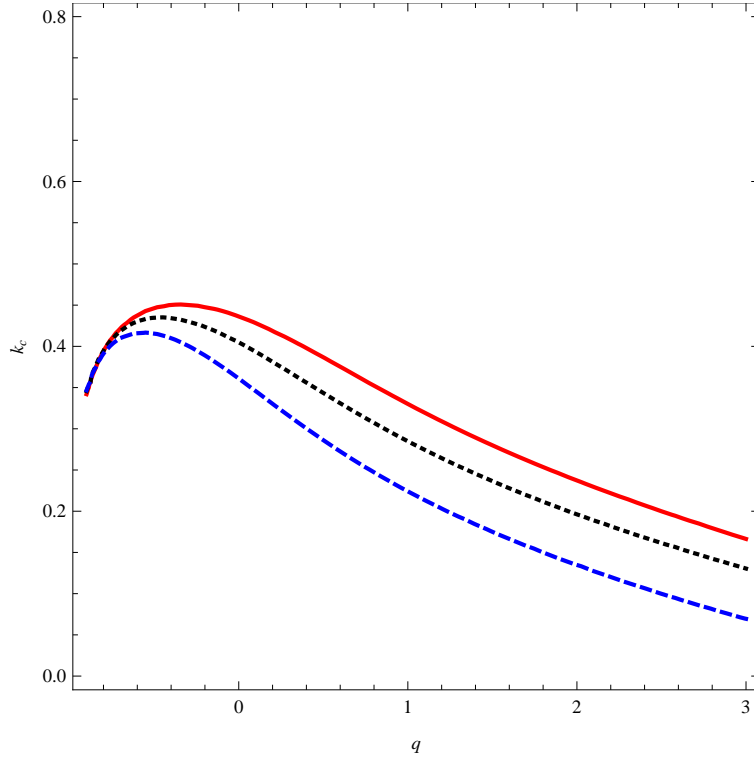


FIG. 6: (Color online) Variation of the critical wave number k_c with the q -nonextensive parameter for different values of μ with $M = 2.10$. Solid curve corresponds to $\mu = 0.5$; dotted curve to $\mu = 0.6$ and dashed curve to $\mu = 0.7$.

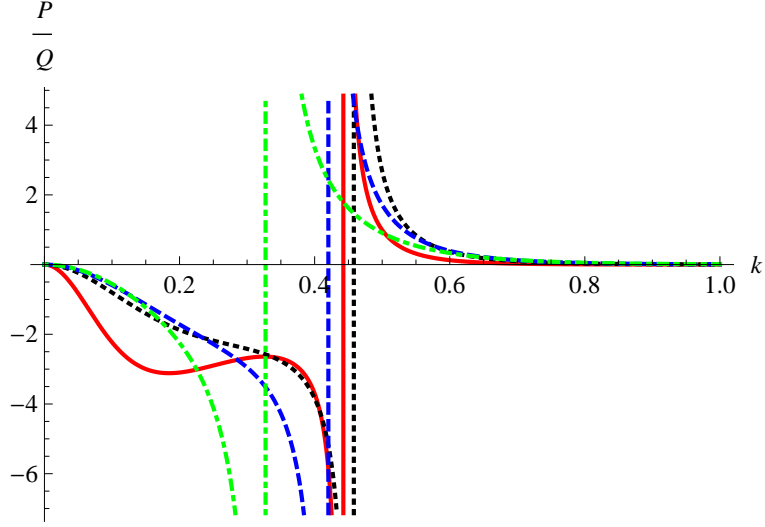


FIG. 7: (Color online) Variation of the ratio P/Q with the carrier wave number k for different values of the q -nonextensive parameter with $\mu = 0.5$ for $Xe^+ - SF_6^-$ plasma ($M = \frac{131}{146} \simeq 0.89$). Solid curve corresponds to $q = -0.7$; dotted curve to $q = -0.3$; dashed curve to $q = 0$ and dotted-dashed curve to $q = 0.4$.

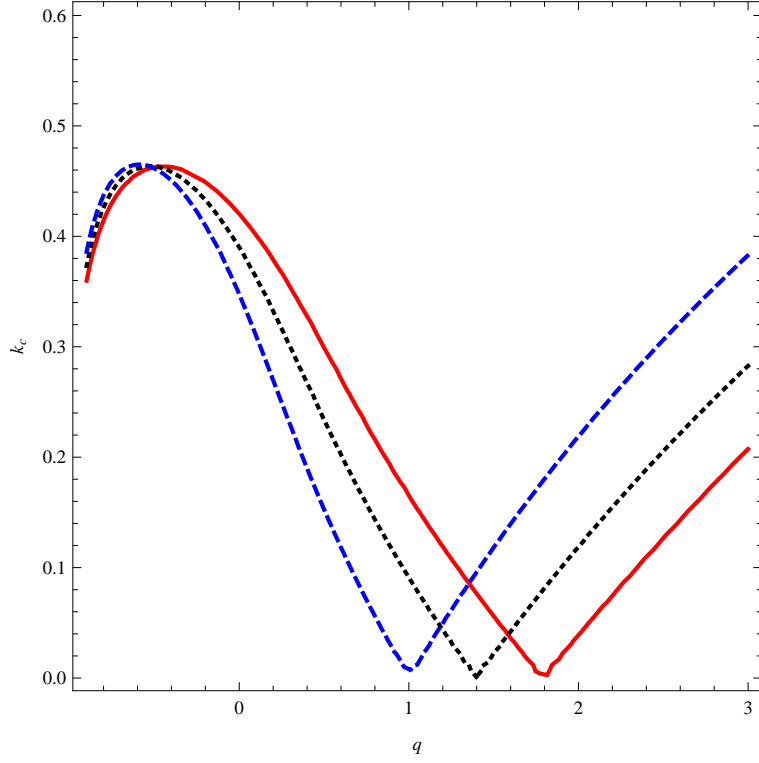


FIG. 8: (Color online) Variation of the critical wave number k_c with the q -nonextensive parameter for different values of μ with $M = 0.89$. Solid curve corresponds to $\mu = 0.5$; dotted curve to $\mu = 0.6$ and dashed curve to $\mu = 0.7$.